doi: 10.1111/j.1365-3121.2006.00715.x

Jurassic-to-present thermal history of the central High Atlas (Morocco) assessed by low-temperature thermochronology

Luis Barbero,[1] Antonio Teixell,[2] María-Luisa Arboleya,[2] Pedro del Río,[1] Peter W. Reiners[3] and Blaid Bougadir[4]

[1]*Departamento de Geología, Universidad de Cádiz, 11510 Puerto Real, Cádiz, Spain;* [2]*Departament de Geologia, Universitat Autònoma de Barcelona, 08193 Bellaterra, Spain;* [3]*Department of Geology and Geophysics, Yale University, New Haven, CT, USA;* [4]*Faculté des Science et Techniques, Université Cadi Ayyad, Marrakech, Morocco*

ABSTRACT

Apatite fission track (AFT) and (U–Th)/He data from the High Atlas have been obtained for the first time to constrain the tectono-thermal evolution of the central part of the chain. Results from Palaeozoic basement massifs indicate long residence at low temperatures, consistently with their original location out of the deepest Mesozoic rift troughs and indicating minor exhumation. The best rocks for extracting the Alpine history of the Atlas Mountains are Jurassic intrusives, which yield AFT ages centred on *c.* 80 Ma; thermal models based on AFT data and constrained by (U–Th)/He suggest that these ages are included in a slow cooling trend from intrusion age to *c.* 50 Ma ago that we attribute to post-rift thermal relaxation. This is followed by a stability period of *c.* 30 Ma and then by a final exhumational cooling until present exposure. Eocene intrusives yield AFT ages similar to those of Rb–Sr and K–Ar suggesting rapid emplacement in the uppermost crust.

Terra Nova, 19, 58–64, 2007

Introduction

The Atlas Mountains represent the most significant relief in North Africa. They extend from Morocco towards Algeria and Tunisia along 2000 km, attaining elevations up to 4000 m. Two branches can be distinguished in Morocco: the NE-trending Middle Atlas and the ENE-trending High Atlas (Fig. 1), which attains the highest altitudes. Traditionally, the Atlas Mountains have been considered intracontinental chains because they are located far from collisional zones and because of the lack of fold nappe structures, regional metamorphism, granitoid intrusions and other features typical of interplate orogens.

Several studies have focused on various aspects of the Atlas structure and evolution, from rift or transcurrent sedimentary troughs during the Mesozoic, to compressional belts of tectonic inversion in Cenozoic to present times (Choubert and Faure-Muret, 1962; Mattauer *et al*., 1977; Laville, 1988; Frizon de Lamotte *et al*., 2000; Piqué *et al*., 2000; Teixell *et al*., 2003; Arboleya *et al*., 2004). The Atlas experienced moderate crustal shortening and exhumation, despite their high elevation (see structural style in Fig. 2). Accordingly, crustal thickening is modest (Wigger *et al*., 1992; Ayarza *et al*., 2005), and the Atlas uplift has been partly attributed to mantle causes (Teixell *et al*., 2003, 2005; Zeyen *et al*., 2005).

The timing of the uplift in the Moroccan Atlas Mountains is still poorly constrained and constitutes a matter of debate. Gomez *et al*. (2000, 2002) and Laville (2002) recently argued on the chronology of folding and uplift. Laville (2002), following Mattauer *et al*. (1977) and Laville and Piqué (1992), argued that total shortening includes a: (a) pre-Cretaceous component resulting in folding, cleavage and erosion of Jurassic igneous and sedimentary rocks; and (b) late Cretaceous to Miocene component responsible for rapid uplift of the High Atlas and for basin development to the south of the chain. On the other hand, Gomez *et al*. (2000, 2002) considered that the shortening of the Moroccan Atlas is the entire result of Cenozoic plate convergence, with no significant pre-Cretaceous shortening. With regard to the main Cenozoic deformation and uplift, several authors have proposed different phases on the basis of syntectonic sediments; their ages range between the late Eocene and the Quaternary (Fraissinet *et al*., 1988; Görler *et al*., 1988; El Harfi *et al*., 1996; Frizon de Lamotte *et al*., 2000; Morel *et al*., 2000).

Apatite fission track (AFT) analysis combined with (U–Th)/He chronology can be a powerful tool to unravel exhumation and uplift histories of orogens (Gallagher *et al*., 1998). To shed more light on the history of the shortening and exhumation of the central High Atlas Mountains, we have performed, for the first time, FT and (U–Th)/He dating in apatite crystals recovered from Palaeozoic to Jurassic supracrustal igneous complexes and sedimentary rocks of this mountain chain.

Summary of geological framework

The Atlas Mountains derive from earlier intracontinental basins, filled with thick sedimentary deposits from the Triassic to the late Cretaceous and affected by episodic magmatic events (see summaries in Choubert and Faure-Muret, 1962 and Piqué *et al*., 2000). Pre-Mesozoic rocks, cropping out in the margins of the High and Middle Atlas and in sparse internal massifs (Fig. 1), were previously affected by the Hercynian orogeny.

During much of the Mesozoic, the High Atlas experienced extension and

Correspondence: Dr Luis Barbero, Departamento de Geología, Facultad Ciencias del Mar y Ambientales, Universidad de Cádiz, Campus de Puerto Real, 11510 Puerto Real, Cádiz, Spain. Tel.: +34 956 016279; fax: +34 956 016797; e-mail: luis.barbero@uca.es

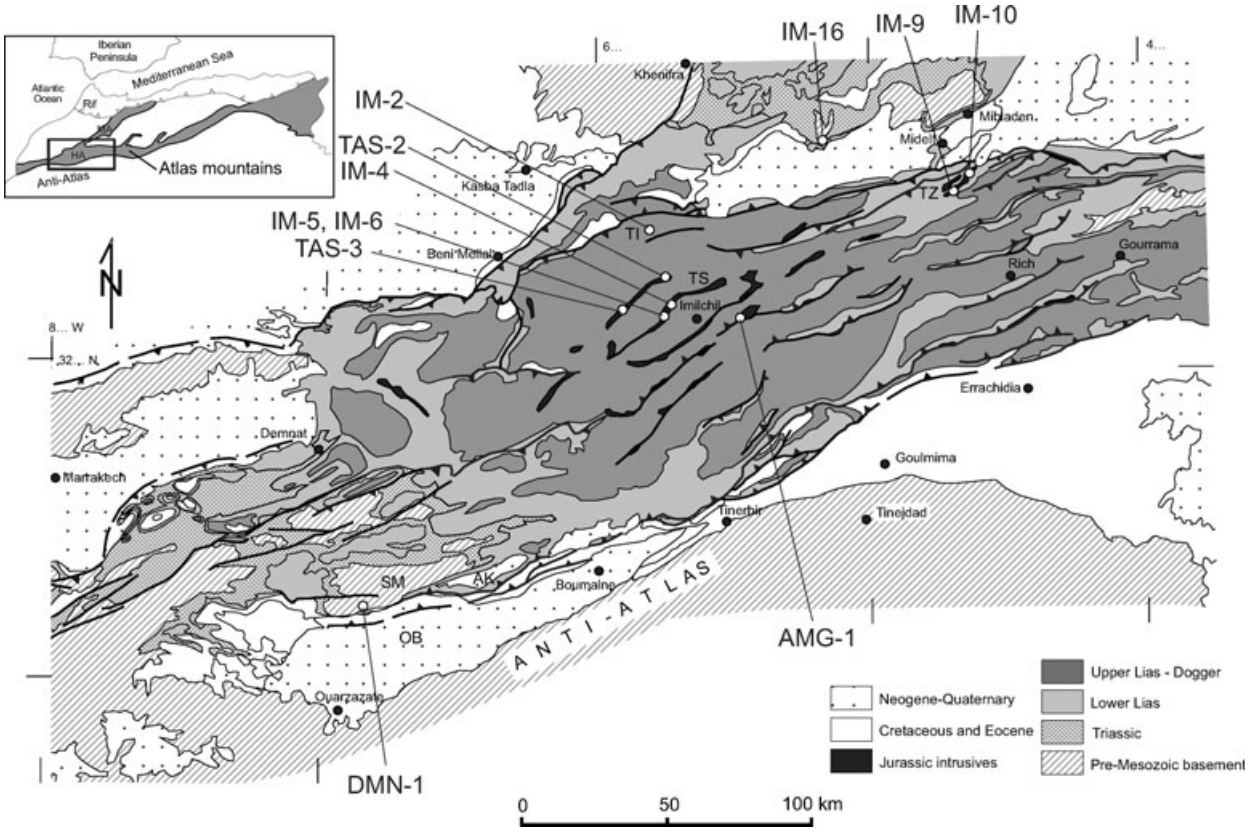

Fig. 1 Geological map of the Central High Atlas (Teixell *et al.*, 2003) showing the location of samples. SM, Skoura massif; OB, Ouarzazate basin; AK, Aït Kandoula basin; TZ, Tamazerht massif; TS, Tassent massif; TI, Tizi n'Isly syncline. Inset shows the location of the Atlas Mountains in the North African foreland (HA, High Atlas; MA, Middle Atlas).

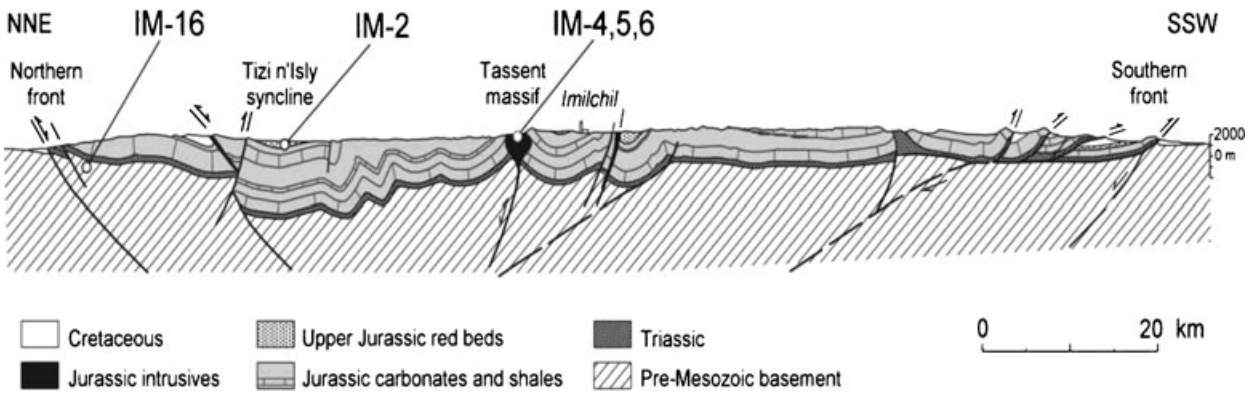

Fig. 2 Cross-section through the High Atlas in the Imilchil region indicating the structural location of the Jurassic intrusive, the Jurassic red bed samples, and the projected position of sample IM-16 (section after Teixell *et al.*, 2003). See location in Fig. 1.

rifting. The first rifting period occurred during the Triassic as evidenced by thick red beds and by a basaltic magmatic episode. A post-rift Liassic platform was drowned and disrupted during the late Liassic–Dogger by a renewed rifting episode (Warme, 1988), and subsiding basins started to differentiate, essentially coinciding with the present day High and Middle Atlas. Up to 5000 m of marls, calciturbites and reefal limestones were accumulated from Toarcian to Bajonian times in central High Atlas. Red beds indicating generalized filling and regression became widespread during the Bathonian. Crustal thinning led to alkaline magmatism, whose manifestations crop out along the axis of the central High Atlas (Figs 1 and 2). Three magmatic formations can be distinguished (Laville and Harmand, 1982; Beraâouz *et al.*, 1994): (a) epizonal plutonic complexes emplaced along the main fault zones at pressures < 1.5 kbar (Lhachmi *et al.*, 2001), mainly composed of

cumulate rocks and syenites-monzodiorites; (b) olivine dolerite dykes, which feed sills intercalated within mid-Jurassic deposits; and (c) plateau basalts produced by fissural volcanism. K–Ar radiometric ages of the Mesozoic intrusions of the High Atlas are compiled in Laville and Harmand (1982) and range from 119 to 173 Ma. Mattauer *et al.* (1977) and Laville and Piqué (1992) proposed that in the late Jurassic there was a major phase of transpressional folding and erosion.

The Cretaceous is represented by a basal red bed formation followed by a platform limestone of Cenomanian–Turonian age; both units either cover the earlier Jurassic deposits or overlap the basement to the N and S of the High Atlas (Figs 1 and 2), being interpreted as post-rift deposits (Teixell *et al.*, 2003). The uppermost Cretaceous consists of fine-grained red beds which according to some authors are coeval with the beginning of the Alpine compression (Laville *et al.*, 1977; Froitzheim *et al.*, 1988; Amrhar, 1995), although in any case deformation was minor and not widespread at that time. A Maastrichtian to middle Eocene marine limestone, now preserved in sparse synclines, is transgressive over the red beds and also records mild and local fold structures. Upper Eocene to Pliocene continental deposits are contemporaneous to the main compression (see references above). There is also abundant magmatism of Cenozoic age, of alkaline to hyperalkaline affinity, composed of volcanic (basalts to phonolites) and minor subvolcanic rocks (syenites with associated carbonatites), clustered into two age groups: 40–45 and 15–0.5 Ma (Tisserant *et al.*, 1976; Harmand and Cantagrel, 1984; Berrahma and Hernandez, 1985; El Azzouzi *et al.*, 1999). This magmatism has been attributed to a mantle upwelling occurring synchronically with the Atlas compression (Teixell *et al.*, 2005).

Methods and results

Samples for thermochronological analysis were collected from diverse rock types in the central High Atlas (Fig. 1). These include granitic and porphyritic intrusions within Palaeozoic basement (IM-16 and DMN-1), late Jurassic to early Cretaceous detrital red beds (IM-2) Jurassic syenites (IM-4–IM-6, TAS-1 and TAS-3, AMG-1), and Eocene syenites (IM-9 and IM-10). FT and (U–Th)/He analyses in apatite crystals were carried out in the University of Cádiz Fission Track Laboratory and Yale University Thermochronometry Laboratory respectively. The analytical methods are described in Barbero *et al.* (2005) and Mitchell and Reiners (2003).

In the (U–Th)/He system in apatites, He is partially accumulated in the crystal lattice when the temperature is between 40 and 90 °C (Farley, 2000). This range is known as He partial retention zone. Although He continues to diffuse out at slow rates at temperatures outside this range, at higher temperatures ($T_c = 80$ °C for usual cooling rates; Farley, 2000) most He is lost by diffusion. If the temperature is lower than 40 °C most of the He is retained. For the FT system, the uppermost limit of the partial annealing zone for a Durango-type composition apatite (0.4 wt % Cl) cooled at a rate of 5 °C Ma^{-1}, is *c.* 108 °C (Brandon *et al.*, 1998).

Sample description, FT and (U–Th)/He data are presented in Tables 1 and 2. Samples from Palaeozoic blocks to the north and south of the High Atlas (Fig. 1) show AFT ages of 270 and 143 Ma; average track length in the former is 11.59 μm, being slightly negatively skewed. The D_{par} values (Table 2) vary from 1.61 to 1.80 μm. AFT ages in the red bed sample could be resolved, on the basis of binomial peak-fit procedures (Brandon, 1992, 1996), into two peaks, at 165 and 295 Ma. AFT ages of Jurassic syenites from the Imilchil area range from 73 to 92 Ma, most showing very low dispersion (chi-squared test passed; Galbraith, 1981). Track lengths measured range from 12.81 to 13.85 μm, the histograms being negatively skewed. The D_{par} values measured vary from 1.62 to 2.22 μm and no correlation with grain age has been found in any case. Finally, Eocene syenites from the Tamazerht massif near Midelt (Fig. 1) yield AFT ages of 50–52 Ma. Track lengths are 13.85-μm long, although uncertainty is high due to the low number ($n = 15$) of confined tracks found. The D_{par} values in the Eocene syenites vary from 1.60 to 1.80 μm.

The (U–Th)/He replicate ages have been obtained in two clear inclusion-free handpicked apatite single grains for each sample. Ages in the red bed

Table 1 Apatite fission track data.

Sample	Rock type	No. crystals	CN-5 track density ($\times 10^6$ tr cm^{-2}) (tracks counted)	Spontaneous track density ($\times 10^6$ tr cm^{-2}) (tracks counted)	Induced track density ($\times 10^6$ tr cm^{-2}) (tracks counted)	Chi-squared probability (%)	Fission track central age (±1σ) (Ma)	Mean track length (μm) (no. tracks)	SD (μm)	D_{par} (μm) (n)	SD (μm)
IM-2	Jurassic red bed	30	1.038 (4813)	2.148 (1213)	1.533 (866)	0.0	242 ± 20				
IM-4	Jurassic syenite	41	1.085 (5029)	0.198 (309)	0.419 (654)	93.3	87 ± 8	12.91 (82)	2.5	1.62 (145)	0.15
IM-5	Jurassic syenite	32	1.076 (4988)	0.284 (317)	0.646 (721)	95.3	80 ± 6	12.81 (43)	1.9	1.91 (150)	0.09
TAS-3	Jurassic syenite	23	1.074 (4981)	0.474 (642)	0.934 (1265)	99.8	92 ± 4			2.22 (150)	0.33
TAS-2	Jurassic syenite	22	1.100 (4328)	1.334 (324)	2.989 (726)	0.0	80 ± 6				
AMG-1	Jurassic syenite	33	1.192 (4759)	0.299 (307)	0.893 (849)	45.4	76 ± 5				
IM-9	Eocene syenite	20	1.067 (4947)	0.317 (236)	1.208 (899)	14.9	50 ± 4			1.80 (50)	0.20
IM-10	Eocene syenite	23	1.058 (4906)	0.378 (316)	1.289 (1098)	46.0	52 ± 4	13.85 (15)	1.5	1.60 (100)	0.17
DMN-1	Palaeozoic dyke	26	1.105 (5126)	1.553 (992)	2.184 (1395)	10.7	143 ± 10			1.61 (200)	0.17
IM-16	Palaeozoic granite	19	1.102 (5110)	6.298 (3317)	4.274 (2251)	23.5	270 ± 10	11.59 (89)	1.7	1.80 (200)	0.18

Ages determined by external detector method using a zeta value (LB) of 337.8 for dosimeter CN-5.

Table 2 Apatite (U–Th)/He data.

Sample	Rock type	Age	Raw age (Ma)*	Mass (ʋg)	Mwar (ʋm)†	U (p.p.m.)	Th (p.p.m.)	Sm (p.p.m.)	^{4}He (nmol g^{-1})	Corrected age (Ma) ± 2σ*
IM2aA	Red beds	Jurassic	77.2	1.67	30.8	0.8	16.9	328.7	2.17	135.3 ± 14.6
IM2aB	Red beds	Jurassic	20.7	1.06	35.0	27.1	66.1	428.7	4.84	33.4 ± 3.0
IM5aA	Syenite	Jurassic	18.3	2.04	42.0	5.8	17.6	302.0	1.02	27.0 ± 3.4
IM5aB	Syenite	Jurassic	22.4	3.31	43.0	2.9	8.2	125.9	0.61	32.0 ± 4.4
IM4aA	Syenite	Jurassic	24.8	2.47	44.5	3.3	8.9	249.2	0.76	35.5 ± 1.4
IM4aB	Syenite	Jurassic	18.1	3.64	46.2	4.2	10.7	253.5	0.69	25.3 ± 3.2
IM6aA	Syenite	Jurassic	27.5	1.06	39.7	5.9	24.8	291.1	1.80	43.4 ± 1.8
IM6aB	Syenite	Jurassic	19.3	1.04	32.5	4.5	14.4	245.0	0.85	32.1 ± 0.9
IM9aA	Syenite	Eocene	9.4	1.50	33.0	7.3	51.0	111.1	0.99	15.3 ± 1.2
IM9aB	Syenite	Eocene	6.6	4.41	50.7	8.7	76.4	148.4	0.96	9.0 ± 0.4
IM10aA	Syenite	Eocene	12.1	7.36	74.7	11.6	144.0	86.3	2.98	15.3 ± 0.6
IM10aB	Syenite	Eocene	27.3	3.66	55.5	1.1	104.8	110.3	3.85	37.6 ± 1.5

*Mass weighted average radius.

†Raw ages were corrected for He loss by α-ejection at the rims of the grains (Farley *et al.*, 1996).

are markedly spread (135 and 33 Ma). In Jurassic syenites, (U–Th)/He ages spread from 25 to 43 Ma. In all cases, two different single-grain replicate ages are clearly different, the maximum difference being of 11 Ma (sample IM-6). The (U–Th)/He ages of Eocene syenites vary from 9 to 38 Ma, replicates being also different (Table 2).

Thermal models and discussion

Modelling procedures can be used to quantitatively evaluate the thermal history of a rock, finding a range of cooling paths compatible with the measured FT data (Gallagher, 1995; Willet, 1997; Ketcham *et al.*, 2000). In the present work, inverse modelling was performed using Ketcham's AFTSolve (Ketcham *et al.*, 2000), which generates random T-t paths using a Monte Carlo algorithm. Estimated ages and track length values were calculated according to the annealing model of Laslett *et al.* (1987) as the measured D_{par} values point to low chlorine compositions similar to Durango apatite (Barbarand *et al.*, 2003). Modelling benefited from external constraints that included the intrusion age of the Jurassic igneous massifs of the High Atlas provided by Hailwood and Mitchell (1971), the (U–Th)/He ages and the age of sedimentary deposits directly overlying the Palaeozoic basement.

The 270 Ma AFT age obtained in sample IM-16, located originally out of the main rift basin, indicates that this region has remained, most of the time, within the first 2–3 km below surface since its late-Hercynian exhumation. This is further confirmed by their track length distribution and by modelling results (Fig. 3), which show a progressive cooling after intrusion reaching the surface by Triassic times, followed by slow heating to a maximum temperature of *c.* 80 °C attained at 40–50 Ma. On the absence of Palaeogene sediments in the area, maximum heating could be caused by thermal disruption related to a regional thermal anomaly that produced volcanic–subvolcanic occurrences of this age in some parts of the eastern Atlasic domain (Taourit, Rekkame and Tamazerht; Tisserant *et al.*, 1976; Rachdi *et al.*, 1997; a thermal event causing uplift and transition from marine to terrestrial environment in this domain was suggested by Teixell *et al.*, 2005). Finally, a cooling episode from *c.* 40 Ma to present is observed. With regard to sample DMN-1, a dyke hosted in the Palaeozoic Skoura massif at the southern margin of the High Atlas (Fig. 1), the AFT age of 143 Ma is close to that of the Jurassic magmatic event, and indicates a long residence at temperatures below the apatite partial annealing zone (APAZ) after supracrustal intrusion, in agreement with the location of the area out of the deep rift trough, similar to sample IM-16.

The detrital sample IM-2 presents two age components that are older than or contemporaneous with the late Jurassic to early Cretaceous depositional age, implying that they have never been reset above the APAZ since erosion of source areas. Although this sample belongs to the deep Jurassic basin (Tizzi n'Isly syncline), its stratigraphic position high in the basin fill and the absence of nappe stacking (Fig. 2) accounts for its long residence at low temperatures. The two age components must represent an inherited thermal signal from source areas, which are likely the Palaeozoic massifs or the Triassic sediments.

AFT ages in the Jurassic syenitic massifs of the Imilchil area fall in the late Cretaceous (Table 1); age values and track lengths allowed thermal modelling to be performed in two samples (Fig. 3). On the other hand, the inter- and intrasample spread in (U–Th)/He ages could be indicative of long-term residence within the (U–Th)/He retention zone or of slow cooling (Fitzgerald *et al.*, 2006). There are several factors which may contribute to (U–Th)/He age dispersion, such as U–Th-rich microinclusions in apatite crystals, fluid inclusions, compositional zoning, variation in crystal size, α-particle ejection correction, He implantation and ^{147}Sm-derived α-particles. Although some of them cannot definitely be disregarded (the presence of microinclusions or fluid inclusions), in our case, He implantation can be ruled out as Sm has been measured and corrections applied (see Table 2).

The recorded AFT ages in the Jurassic syenites coincide with the age of the onset of Alpine compression in the Atlas region according to the previously cited authors; however, thermal modelling shows a continuous and steady cooling from K–Ar closure temperature at *c.* 140 Ma to

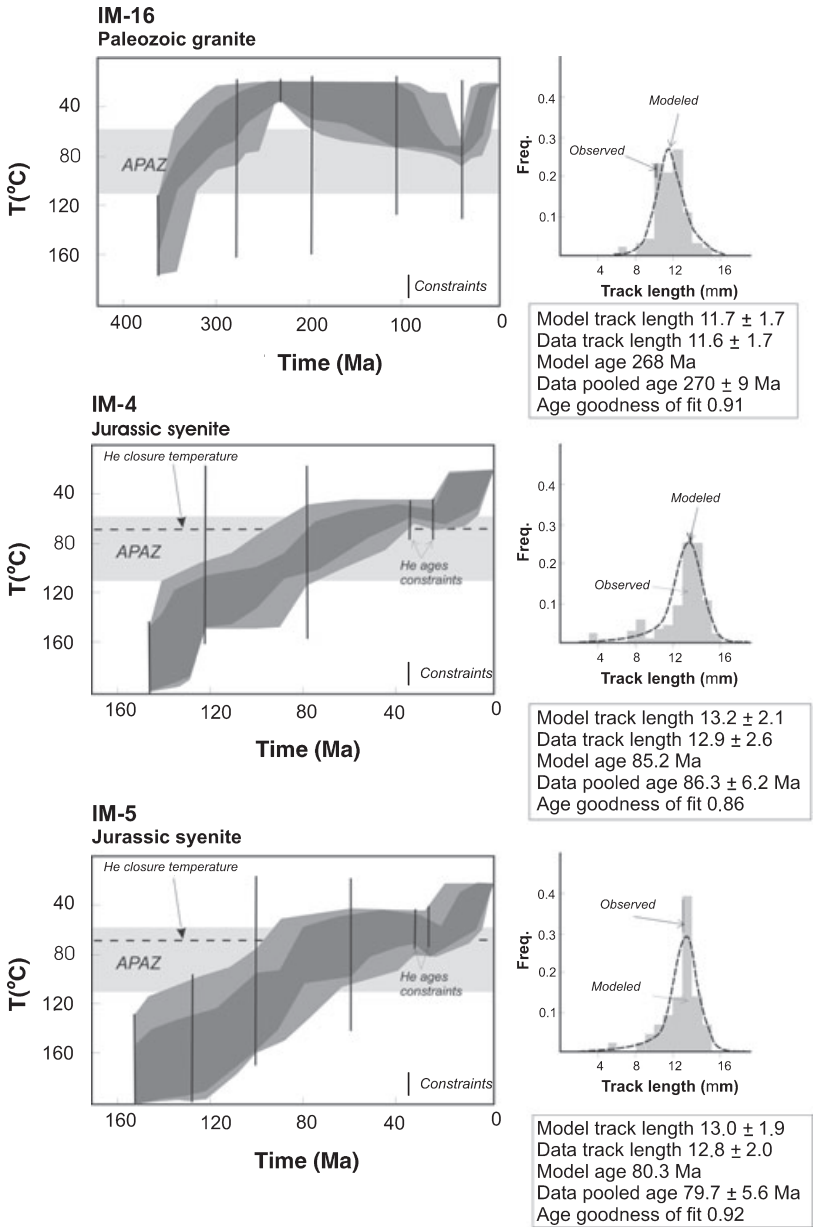

Fig. 3 Thermal models from samples IM-16, IM-4 and IM-5. K–Ar ages used as constraints for the gabbros of the Tassent massif vary from 119 ± 3 (whole rock) to 160 ± 3 (biotite) (Hailwood and Mitchell, 1971).

temperatures around 60 °C at *c.* 50 Ma. A slow cooling rate of 0.75–1.5 °C Ma^{-1} is deduced for this period. Geological evidence for contemporaneous denudation is lacking. In fact, there is a sedimentary record (first of fluvial deposits of early Cretaceous age and then of platform limestones of Cenomanian–Turonian age) indicative of slow and homogeneous subsidence following the Jurassic rifting episode. Late Cretaceous red beds and Maastrichtian to Eocene limestones, although claimed to be contemporaneous with compression, still record slow subsidence, and regionally significant deformation or erosion did not occur. Hence, we interpret the slow cooling trend as a combination of post-magmatic cooling and post-rift thermal relaxation, the individual AFT ages obtained not reflecting any tectonically driven exhumation. Thermokinematic models (Bertotti *et al.*, 1999) have shown that in rifting scenarios absolute ages may not be directly related to deformation, but controlled by the downward movement of isotherms. Cooling slowed down markedly *c.* 50 Ma ago, leaving the samples residing at approximately 70 °C until *c.* 20 Ma ago (Fig. 3). (U–Th)/He data constrain the validity of the period of thermal stability resulting from AFT modelling (Fig. 3). This thermal stability suggests that the Atlas Mountains remained in tectonic quiescence, and the flattening of the cooling path reflect the decay of the rift thermal anomaly and/or the distant effect of the Palaeogene magmatism. In the past 20 Ma, rapid cooling from 60 °C to present surface temperature coincides with a large coarse-grained sediment influx into the adjacent fore deeps, such as the Ouarzazate and Aït Kandoula basins, attributed to the early Miocene (Görler *et al.*, 1988; Benammi and Jaeger, 2001; Tesón, 2005).

An additional conclusion that can be drawn from these results is that during the late Jurassic to early Cretaceous times the sampled Jurassic syenite massifs reside at temperatures close to or above the upper limit of the APAZ and were not exposed at surface. This result does not favour the late Jurassic shortening and erosion phase claimed by some authors. The inference of such a deformation phase was based on the presence of red beds of supposed Cretaceous age and unconformable attitude on top of the Jurassic igneous massifs, which presently occupy the core of kilometric-scale anticlines (Laville and Piqué, 1992). However, these red beds are never seen overlapping the Jurassic sedimentary layers in the anticline flanks, and their geometry suggests that they may be fragments of the Triassic wall rock embedded within the magmatic bodies.

The Eocene syenite of Tamazerth yield AFT ages of 50–52 Ma that although slightly older than previously published Rb–Sr (44 ± 4 Ma) and K–Ar (42 ± 3 Ma) ages (Tisserant *et al.*, 1976), confirm that they belong to a different magmatic group from those of the Imilchil area, and suggest that they intruded rapidly in very shallow crustal levels. Thermal modelling has not been possible due to the scarcity of confined horizontal tracks.

Conclusions

The AFT and (U–Th)/He results presented in this work constitute the first thermochronological dataset for the Atlas Mountains of North Africa. Samples from Palaeozoic massifs record old ages implying that the present exposure of the basement massifs within the Atlas Mountains does not imply large amounts of Alpine exhumation, but the massifs have resided close to surface from the Mesozoic until present. To unravel the Cenozoic thermal history related to mountain building in the central part of the High Atlas, it has been necessary to study of the Jurassic igneous intrusives. The main results from dating and modelling in the latter indicate a slow period of cooling from intrusion time to *c*. 50 Ma, attributable to post-magmatic and post-rift thermal relaxation, and preclude any significant uplift and erosion in late Jurassic times. This cooling period was followed by an interval of stability until *c*. 20 Ma, when thermochronological and sedimentary data record the main uplift and erosional phase of the central High Atlas.

Acknowledgements

The authors thank J. Barbarand and J. Honnorez for their helpful revision of the manuscript. We thank E. Tesón, B. Igmoullan and R. Vela for assistance in the collection and preparation of some of the samples. This work has been supported by MCYT project BTE-2003-00499, NATO grant CLG980144, AECI project 23P/00 and by the Consolider-Ingenio 2010 Programme under project CSD2006-0041 'TOPO-IBERIA'. This research is part of the objectives of the Junta de Andalucía PAI group RNM-160.

References

Amrhar, M., 1995. *Tectonique et inversions géodynamiques post-rift dans le Haut Atlas occidental: structures, instabilités tectoniques et magmatismes liés a l'ouverture de l'Atlantique central et la collision Afrique-Europe*. PhD thesis. University of Cadi Ayyad, Marrakech, Morocco.

Arboleya, M.-L., Teixell, A., Charroud, M. and Julivert, M., 2004. A structural transect of the High and Middle Atlas of Morocco. *J. Afr. Earth Sci.*, **39**, 319–327.

Ayarza, P., Alvarez-Lobato, F., Teixell, A., Arboleya, M.-L., Tesón, E., Julivert, M. and Charroud, M., 2005. Crustal structure under the central High Atlas Mountains (Morocco) from Geological and gravity data. *Tectonophysics*, **400**, 67–84.

Barbarand, J., Carter, A., Wood, I. and Hurford, T., 2003. Compositional and structural control of fission-track annealing in apatite. *Chem. Geol.*, **198**, 107–137.

Barbero, L., Glasmacher, U.A., Villaseca, C., López García, J.A. and Martín-Romera, C., 2005. Long-term thermotectonic evolution of the Montes de Toledo area (Central Hercynian Belt, Spain): constraints from apatite fission track analysis. *Int. J. Earth Sci.*, **94**, 193–203.

Benammi, M. and Jaeger, J.-J., 2001. Magnetostratigraphy and palaeontology of the continental Middle Miocene of the Aït Kandoula Basin, Morocco. *J. Afr. Earth Sci.*, **33**, 335–348.

Beraâouz, E.H., Platevoet, B. and Bonin, B., 1994. Le magmatisme mésozoïque du Haut-Atlas (Maroc) et l'ouverture de l'Atlantique central. *C. R. Acad. Sci. Paris*, **318**, 1079–1085.

Berrahma, M. and Hernandez, J., 1985. Nouvelles données sur le volcanisme trachytique hyperalcalin du volcan du Siroua (Anti-Atlas, Maroc). *C. R. Acad. Sci. Paris*, **300**, 863–868.

Bertotti, G., Seward, D., Wijbrans, J., ter Voorde, M. and Hurford, A.J., 1999. Crustal thermal regime prior to, during, and after rifting: a geochronological and modelling study of the Mesozoic South Alpine rifted margin. *Tectonics*, **18**, 185–200.

Brandon, M.T., 1992. Decomposition of fission-track grain-age distributions. *Am. J. Sci.*, **292**, 535–564.

Brandon, M.T., 1996. Probability density plot for fission-track grain-age samples. *Radiat. Meas.*, **26**, 663–676.

Brandon, M.T., Roden, T.M.K. and Garver, J.I., 1998. Late Cenozoic exhumation of the Cascadia accretionary wedge in the Olympic Mountains, Northwest Washington State. *Geol. Soc. Am. Bull.*, **110**, 985–1009.

Choubert, G. and Faure-Muret, A., 1962. Evolution du domaine atlasique marocain depuis les temps paléozoïques. In: *Livre a la Mémoire du Professeur Paul Fallot, Mem. hors Sér*, Vol. 1, pp. 447–527. Soc. Géol de Fr. Paris.

El Azzouzi, M., Bernard-Griths, J., Bellon, H., Maury, R.C., Piqué, A., Fourcade, S., Cotten, J. and Hernandez, J., 1999. Evolution des sources du volcanisme marocain au cours du Néogène. *C. R. Acad. Sci. Paris*, **329**, 95–102.

El Harfi, A., Lang, J. and Salomon, J., 1996. Le remplissage continental cénozoïque du bassin d'avant-pays de Ouarzazate. Implications sur l'évolution géodynamique du Haut-Atlas Central (Maroc). *C. R. Acad. Sci. Paris*, **323**, 623–630.

Farley, K.A., 2000. Hellium difusion from apatite: general behaviour as illustrated by Durango fluorapatite. *J. Geophys. Res.*, **105**, 2903–2914.

Farley, K.A., Wolf, R.A. and Silver, L.T., 1996. The effects of long alpha-stopping distances on (U–Th)/He ages. *Geochim. Cosmochim. Acta*, **60**, 4223–4229.

Fitzgerald, P.G., Baldwin, S.L., Webb, L.E. and O'Sullivan, P.B., 2006. Interpretation of (U–Th)/He single grain ages from slowly cooled crustal terranes: a case study from the Transantartic Mountains of Southern Victoria Land. *Chem. Geol.*, **225**, 91–120.

Fraissinet, C.E., Zouine, M., Morel, J.-L., Poisson, A., Andrieux, J. and Faure-Muret, A., 1988. Structural evolution of the southern and northern central High Atlas in Paleogene and Mio-Pliocene times. In: *The Atlas System of Morocco* (V. Jacobshagen, ed.), pp. 273–291. Springer-Verlag, Berlin.

Frizon de Lamotte, D., Saint Bezar, B., Bracène, E. and Mercier, E., 2000. The two main steps of the Atlas building and geodynamics of the western Mediterranean. *Tectonics*, **19**, 40–761.

Froitzheim, N., Stets, N. and Wurster, P., 1988. Aspects of western High Atlas tectonics. In: *The Atlas System of Morocco* (V. Jacobshagen, ed.), pp. 219–244. Springer-Verlag, Berlin.

Galbraith, R.F., 1981. On statistical models of fission track counts. *Math. Geol.*, **13**, 471–478.

Gallagher, K., 1995. Evolving temperature histories from apatite fission-track data. *Earth Planet. Sci. Lett.*, **136**, 421–435.

Gallagher, K., Brown, R.W. and Johnson, C.J., 1998. Geological applications of fission track analysis. *Annu. Rev. Earth Planet. Sci.*, **26**, 519–572.

Gomez, F., Beauchamp, W. and Barazangi, M., 2000. Role of Atlas Mountains (northwest Africa) with the African-Eurasian plate-boundary zone. *Geology*, **28**, 775–778.

Gomez, F., Beauchamp, W. and Barazangi, M., 2002. Role of Atlas Mountains (northwest Africa) within the African-Eurasian plate-boundary zone: reply. *Geology*, **30**, 96.

Görler, K., Helmdach, F.-F., Gaemers, P., Heissig, K., Hinsch, W., Mädler, K., Schwarzhans, W. and Zucht, M., 1988. The uplift of the central High Atlas as deduced from Neogene continental sediments of the Ouarzazate province, Morocco. In: *The Atlas System of Morocco* (V. Jacobshagen, ed.), pp. 361–404. Springer-Verlag, Berlin.

Hailwood, E.A. and Mitchell, J.C., 1971. Paleomagnetic and radiometric dating results from Jurassic intrusions in south

Morocco. *Geophys. J. R. Astron. Soc.*, **24**, 351–364.
Harmand, C. and Cantagrel, J.M., 1984. Le volcanisme alcalin Tertiaire et Quaternaire du Moyen Atlas (Maroc): chronologie K/Ar et cadre géodynamique. *J. Afr. Earth Sci.*, **2**, 51–55.
Ketcham, R.A., Donelick, R.A. and Carlson, W.D., 2000. AFTSolve: a program for multi-kinetic modeling of apatite fission-track data. *Geol. Mat. Res.*, **2**, 1–32.
Laslett, G.M., Green, P.F., Duddy, I.R. and Gleadow, A.J.W., 1987. Thermal annealing of fission tracks in apatite: 2. A quantitative analysis. *Chem. Geol.*, **65**, 1–13.
Laville, E., 1988. A multiple releasing and restraining stepover model for the Jurassic strike-slip basin of the central High Atlas (Morocco). In: *Triassic-Jurassic Rifting: Continental Breakup and the Origin of the Atlantic Ocean and Passive Margins* (W. Mainspeizer, ed.), pp. 499–523. Elsevier, New York, NY.
Laville, E., 2002. Role of Atlas Mountains (northwest Africa) within the African-Eurasian plate-boundary zone: comment. *Geology*, **30**, 95.
Laville, E. and Harmand, C., 1982. Évolution magmatique et tectonique du bassin intracontinental mésozoïque du Haut Atlas (Maroc): un modèle de mise en place synsédimentaire de massifs 'anorogéniques' liés à des décrochements. *Bull. Soc. Geol. France*, **24**, 213–227.
Laville, E. and Piqué, A., 1992. Jurassic penetrative deformation and Cenozoic uplift in the central High Atlas (Morocco): a tectonic model. Structural and orogenic inversions. *Geol. Rundsch.*, **81**, 157–170.
Laville, E., Lesage, J.-L. and Séguret, M., 1977. Géometrie, cinématique (dynamique) de la tectonique atlasique sur le versant sud du Haut Atlas marocain: Aperçu sur les tectoniques hercyniennes et tardi-hercyniennes. *Bull. Soc. Geol. France.*, **19**, 527–539.
Lhachmi, A., Lorand, J.-P. and Fabries, J., 2001. Pétrologie de l'intrusion alcaline mésozoïque de la région d'Anemzi, Haut Atlas Central, Maroc. *J. Afr. Earth Sci.*, **32**, 741–764.
Mattauer, M., Tapponier, P. and Proust, F., 1977. Sur les mécanismes de formation des chaînes intracontinentales: l'example des chaînes atlasiques du Maroc. *Bull. Soc. Geol. France*, **19**, 521–526.
Mitchell, S.G. and Reiners, P.W., 2003. Influence of wildfire on apatite and zircon (U–Th)/He ages. *Geology*, **31**, 1025–1028.
Morel, J.-L., Zouine, M., Andrieux, J. and Faure-Muret, A., 2000. Déformations néogènes et quaternaires de la bordure nord haut atlasique (Maroc): rôle du socle et conséquences structurales. *J. Afr. Earth Sci.*, **30**, 119–131.
Piqué, A., Charroud, M., Laville, E. and Amrhar, M., 2000. The Tethys southern margin in Morocco: Mesozoic and Cainozoic evolution of the Atlas domain. *Mem. Mus. Natl Hist. Nat.*, **182**, 93–106.
Rachdi, H., Berrahma, M., Delaloye, M., Faure-Muret, A. and Dahmani, M., 1997. Le volcanisme tertiare du Rekkame (Maroc): pétrologie, géochimie et géochronologie. *J. Afr. Earth. Sci.*, **24**, 259–269.
Teixell, A., Arboleya, M-L., Julivert, M. and Charroud, M., 2003. Tectonic shortening and topography in the central High Atlas (Morocco). *Tectonics*, **22**, 1051, doi: 10.1029/2002TC001460.
Teixell, A., Ayarza, P., Zeyen, H., Fernàndez, M. and Arboleya, M-L., 2005. Effects of mantle upwelling in a compressional setting: the Atlas Mountains of Morocco. *Terra Nova*, **17**, 456–461.
Tesón, E., 2005. *Estudio Estructural del Margén sur del Alto Atlas Entre los valles del Dadés y Mgoun*, 79 p. Trabajo de Investigación, Universitat Autònoma de Barcelona, Barcelona.
Tisserant, D., Thuizat, R. and Agard, J., 1976. Donées géochronologiques sur le complexe de roches alcalines du Tamazeght (Haut Atlas de Midelt, Maroc). *Bull. BRGM*, **3**, 279–283.
Warme, J.E., 1988. Jurassic carbonate facies of the Central and Eastern High Atlas rift, Morocco. In: *The Atlas System of Morocco* (V. Jacobshagen, ed.), pp. 169–199. Springer-Verlag, Berlin.
Wigger, P., Asch, G., Giese, P., Heinsohn, W.-D., El Alami, S.O. and Ramdani, F., 1992. Crustal structure along a traverse across the Middle and High Atlas mountains derived from seismic refraction studies. *Geol. Rundsch.*, **81**, 237–248.
Willet, S.D., 1997. Inverse modelling of annealing of fission tracks in apatite: a controlled random search method. *Am. J. Sci.*, **297**, 939–969.
Zeyen, H., Ayarza, P., Fernàndez, M. and Rimi, A., 2005. Lithospheric structure under the western African–European plate boundary: a transect across the Atlas Mountains and the Gulf of Cadiz. *Tectonics*, **24**, TC2001, doi: 10.1029/2004TC001639.

Received 15 March 2006; revised version accepted 2 October 2006

